Magnetic interlayer coupling in ferromagnet/insulator/ferromagnet structures

C. L. Platt
Department of Physics and Center for Magnetic Recording Research, CMRR-0401, University of California–San Diego, La Jolla, California 92093-0401

M. R. McCartney
Center for Solid State Science, Arizona State University, Tempe, Arizona 85287-1704

F. T. Parker
Center for Magnetic Recording Research, CMRR-0401, University of California–San Diego, La Jolla, California 92093-0401

A. E. Berkowitz
Department of Physics and Center for Magnetic Recording Research, CMRR-0401, University of California–San Diego, La Jolla, California 92093-0401

(Received 1 October 1999)

Magnetic coupling between $Co_{50}Fe_{50}$ (CoFe) and $Ni_{81}Fe_{19}$ (NiFe) thin films separated by a SiO_2 layer was investigated with magnetization measurements, Mössbauer spectroscopy, and Lorentz imaging. SiO_2 thicknesses varied from 0 to 1000 Å. When the spacer layer was thicker than 10 Å, separate reversal of the magnetic layers was observed in the hysteresis loops. The coercivity of a 300 Å NiFe film separated from a 300 Å CoFe film by 20 Å of SiO_2 was about 50 Oe, compared to 1 Oe for a free NiFe layer. The coercive field of the NiFe decreased and the magnetization reversal became sharper with increasing SiO_2 thickness. The NiFe showed an enhanced coercivity even with a demagnetized CoFe layer, suggesting that domain walls contribute to the coupling. Mössbauer measurements in zero applied field confirmed that the spin dispersion of the NiFe layer resembled the CoFe dispersion in strongly coupled trilayers, but that the NiFe spins were nearly collinear with the easy axis in trilayers with small coupling. Lorentz imaging of single magnetic layer samples showed a complex, immobile domain-wall structure in the CoFe, but only ripple structure was observed in the NiFe. The Lorentz images of trilayers suggested that magnetostatic coupling between domain walls in the CoFe and induced walls and ripple structure in the NiFe resulted in the enhanced NiFe coercivity.

I. INTRODUCTION

Understanding the nature and extent of magnetic exchange interactions and coupling effects is important for many of the industrial applications of magnetic thin-film devices. In particular, magnetoresistive devices have transport properties that depend on the relative orientation of magnetic moments in neighboring grains or thin film layers. Most investigations have focused on metallic multilayer systems like Fe/Cr (Refs. 1,2) and Co/Cu,[3] where the thickness of nonmagnetic material between the ferromagnetic layers determines whether the interlayer coupling will be ferromagnetic or antiferromagnetic. By varying the thickness, coupling properties can be tailored to meet specific application requirements. Recent interest in spin-dependent tunnel junctions[4] has motivated the study of magnetic coupling across nonmetallic (insulating) materials.[5] In a magnetic tunnel junction, the thin insulating layer minimizes magnetic coupling between the electrodes. Interactions between the electrodes, however, are still present. It has already been demonstrated how the switching behavior of the soft magnetic layer and the magnetic properties of the hard layer can influence each other.[6,7] As device sizes continue to shrink, magnetic coupling and shape anisotropy effects must be taken into account to optimize performance.[8]

The band structure of an insulator minimizes exchange interactions, but other sources of coupling need to be considered (see Fig. 1). Percolation through a very thin layer, such as a tunnel junction barrier, can provide direct coupling between two ferromagnetic films [Fig. 1(a)]. The ''pinhole'' issue is a subject of general importance in investigations of multilayer systems. The transport properties of tunnel junctions will clearly reflect the presence of metallic shorts through the barrier. The influence of these indeterminate pathways on interlayer coupling, however, may be less obvious. So far, direct imaging of these pathways has been difficult. Controlled oxidation experiments have been used to probe the permeable nature of thin metallic layers.[9] Néel[10] proposed that conformal roughness (''orange-peel'') at interfaces can result in ferromagnetic coupling for a moderate thickness of spacer material [Fig. 1(b)]. Recently, an uncorrelated roughness model for biquadratic coupling has been proposed as well.[11] In Néel's model, roughness features on the surface of the bottom ferromagnetic layer propagate through the uppermost layers as they are deposited. Magnetostatic coupling occurs between the roughness features, assuming that the magnetization is uniform and collinear at the interface.[12] Magnetostatic coupling can also exist between domain walls in the two magnetic layers [Fig. 1(c)]. In this case, stray flux fields from walls in one film can influence the magnetization reversal process in the other magnetic layer.[13] Finally, Slonczewski[14] proposed that the change in angular momentum experienced by spin-polarized electrons tunneling across a barrier results in a magnetic exchange coupling

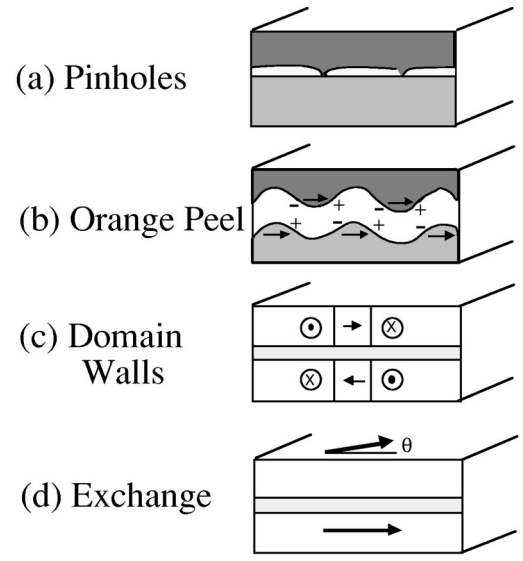

FIG. 1. Possible coupling mechanisms between two ferromagnetic layers separated by an insulating layer.

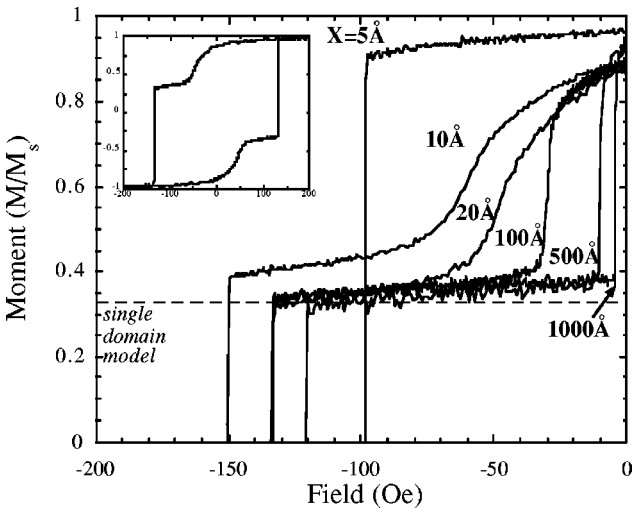

FIG. 2. Magnetization data in the second quadrant for NiFe(300 Å)/$SiO_2(x)$/CoFe(300 Å) trilayers. The inset shows the full hysteresis loop for the sample with a 20 Å spacer. M_s is moment at saturation.

[Fig. 1(d)]. The magnitude and sign of the coupling oscillates depending on the interfacial barrier properties.

In this paper, we report on magnetic coupling effects observed in $Ni_{81}Fe_{19}/SiO_2/Co_{50}Fe_{50}/Si$ multilayer films. The coercive field of a soft $Ni_{81}Fe_{19}$ (NiFe) film was enhanced (relative to a free NiFe film) when separated from a $Co_{50}Fe_{50}$ (CoFe) film by a sputtered SiO_2 spacer layer up to 1000 Å thick. NiFe minor loops showed an enhanced coercivity even in the presence of a demagnetized CoFe layer. Mössbauer measurements confirmed that the remanent spin dispersion of the NiFe layer resembled the CoFe dispersion in strongly coupled trilayers. Determination of magnetic structure by Lorentz transmission electron microscopy (TEM) revealed that low mobility domain walls and ripple structure dominated the magnetization reversal characteristics of free CoFe films. Imaging of trilayer samples showed evidence of domain walls in the NiFe that were not observed in the single films. These results suggest that the immobile domain walls in the CoFe modify the NiFe domain structure to reduce the total magnetostatic energy. The interaction of the stray flux from CoFe walls with induced walls and modified ripple structure in the NiFe inhibits the moment reversal of the NiFe in fields sufficient to switch a free film.

II. SAMPLE PREPARATION

The trilayer samples in this study were grown by magnetron sputtering onto Si(100) substrates at nominal room temperature. The wafers were mounted on a rotating substrate table that passes the wafers over individual sputtering guns. The sputtering gas was 2mTorr of Ar in a background pressure of 2×10^{-7} Torr. The base magnetic layer was 300 Å of $Co_{50}Fe_{50}$ alloy, SiO_2 was the spacer material, and 300 Å of Permalloy ($Ni_{81}Fe_{19}$) was the top magnetic layer. A final 100 Å SiO_2 layer was added as an oxidation barrier. Each magnetic film was dc sputtered from a composite target. The SiO_2 was rf sputtered from an oxide target at 200W. Separate control samples of the magnetic films were made with capping and/or base layers of SiO_2 to reproduce their interface structure in the trilayers. Cross-sectional TEM indicated that these films were uniform and the interfaces were smooth on a scale of about 5 Å. The magnetic films were polycrystalline, and the SiO_2 was amorphous. Magnetization was measured on an alternating gradient magnetometer (AGM) at room temperature and on a superconducting quantum interference device magnetometer at low temperatures. Samples were also prepared on carbon-coated copper TEM grids for Lorentz microscopy. Magnetic imaging was performed for different in-plane fields by tilting the samples in 250–1000 Oe vertical fields.

III. MAGNETIZATION MEASUREMENTS

A. Control samples

The in-plane magnetic properties of the control samples of 300 Å thick CoFe and NiFe films were measured for comparison with the trilayers. The CoFe films exhibited a number of interesting properties, which will be discussed more fully elsewhere.[15] The hysteresis loops taken on the CoFe indicated a sharp switching behavior that was relatively independent of the in-plane applied field direction. Torque measurements in high fields, however, showed a small uniaxial anisotropy ($K_1=1.5\times10^4$ erg/cc). By comparison, the NiFe films showed marked anisotropic magnetization behavior in both hysteresis and torque measurements. These deposition-induced anisotropies may have been caused by stray fields from the magnetron sputtering guns in the vacuum chamber. The coercivity (H_c) along the easy axis of the NiFe film was about 1 Oe. High-field torque measurements showed a uniaxial anisotropy ($K_1=1\times10^3$ erg/cc) with the easy axis in a direction parallel to the easy axis observed in magnetization measurements.

B. Hysteresis response

Figure 2 shows the magnetization data in the second quadrant at room temperature for NiFe(300 Å)/$SiO_2(x)$/CoFe(300 Å) samples with various thicknesses (x) of SiO_2.

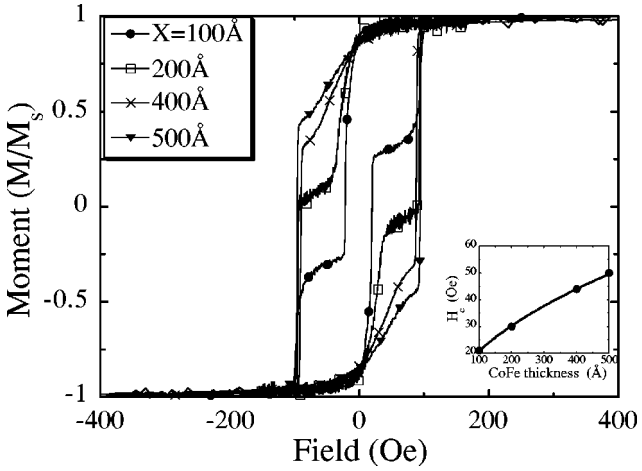

FIG. 3. Hysteresis loops for NiFe(300 Å)/SiO_2(20 Å)/CoFe(x) samples; inset shows H_c(NiFe) as a function of CoFe thickness. The power-law fit is approximately linear with t_{CoFe}.

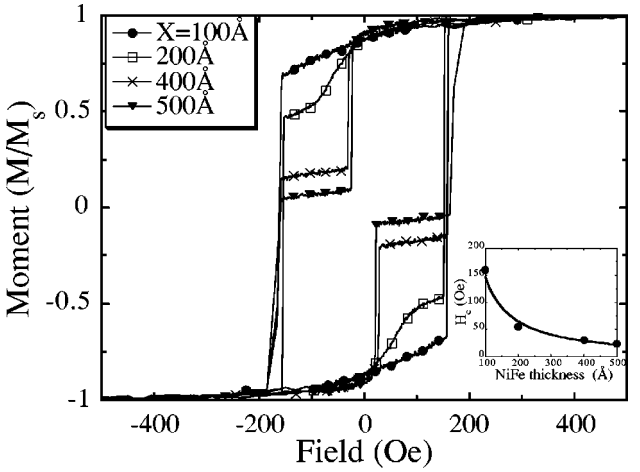

FIG. 4. Hysteresis loops for NiFe(x)/SiO_2(20 Å)/CoFe(300 Å) samples; inset shows H_c(NiFe) as a function of NiFe thickness. The power law fit varies approximately like $1/t_{\mathrm{NiFe}}$.

The inset shows the full hysteresis loop for the sample with a 20 Å spacer. The NiFe switching field, H_c(NiFe), is never larger than the CoFe switching field, H_c(CoFe). The magnetic layers were sufficiently decoupled to observe separate switching behavior at an interlayer thickness of 10 Å. Below this thickness, the SiO_2 layer was probably not continuous, and both layers reversed their moment at the same field. The dashed line in Fig. 2 denotes the approximate magnetization expected, assuming the NiFe moment has reversed completely antiparallel to the CoFe, i.e., in a ''single-domain'' model. Such a model does not accurately describe these data because of magnetic interlayer coupling. The data from the 10 Å spacer sample suggest that not all of the NiFe had reversed before the CoFe switched; however, it is not possible to separate the contributions of each layer to the total magnetization. For spacers 20 Å or thicker, the magnetization gradually approached the dashed line just before the CoFe switched. H_c(NiFe) was about 50 Oe (at the inflection point of the hysteresis loop) when spaced 20 Å from the CoFe, much greater than H_c of a free NiFe film (1 Oe). As the spacer thickness increased, H_c(NiFe) decreased, and the switching became sharper. H_c(CoFe) exhibited no clear trend with SiO_2 thickness. In addition, the coupling effects on the NiFe were not diminished by reversing the order of deposition of the CoFe and NiFe, or by using a backing magnet in an attempt to induce an easy axis in the films during deposition. The easy axis observed in the NiFe control samples was not evident in the hysteresis loop measurements on the trilayers. High-field torque measurements on the trilayers showed a uniaxial anisotropy with the same easy axis as that observed for the free CoFe film. This is a strong indication that the CoFe was dominating the composite magnetic properties of the trilayers.

The relative enhancement of H_c(NiFe) was dependent on the NiFe or CoFe layer thickness. It is known that domain-wall widths change with magnetic film thickness, which has implications for possible wall coupling mechanisms. In general, Néel wall energies increase and wall widths decrease with increasing film thickness.[16] Figure 3 shows the hysteresis loops from a series of trilayers with varying CoFe thickness [NiFe(300 Å)/SiO_2(20 Å)/CoFe(x)] with an inset showing how H_c(NiFe) varied with CoFe thickness (t_{CoFe}). The fit to the data shows a linear increase of H_c(NiFe) with t_{CoFe}. Figure 4 shows the hysteresis loops for a series of trilayers with varying NiFe thickness [NiFe(x)/SiO_2(20 Å)/CoFe(300 Å)] with an inset showing how H_c(NiFe) varied with NiFe thickness (t_{NiFe}). The solid line is a power-law fit to the data which indicates a $1/t_{\mathrm{NiFe}}$ dependence of H_c(NiFe).

Hysteresis loops were also measured at cryogenic temperatures. Figure 5 shows the temperature dependence of H_c(NiFe) and H_c(CoFe) (each 300 Å) in trilayers with 20 and 100 Å of SiO_2 spacer. In both cases, H_c was larger for

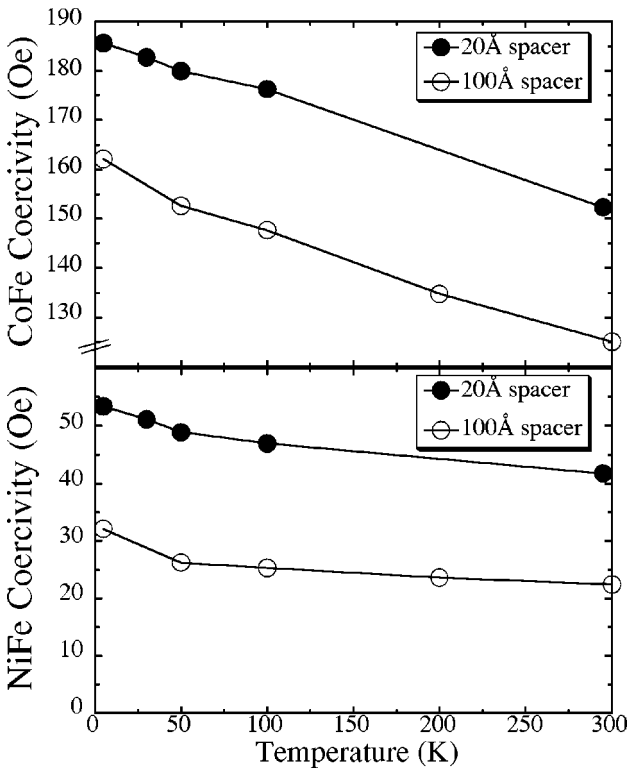

FIG. 5. H_c(CoFe) and H_c(NiFe) vs temperature in trilayers with SiO_2 spacers of 20 and 100 Å.

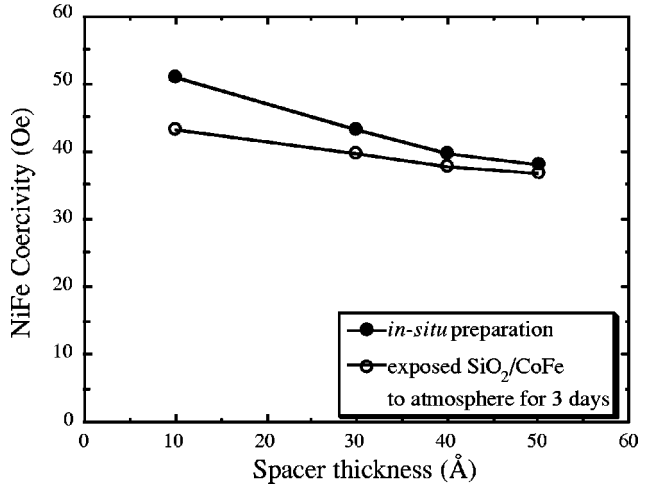

FIG. 6. H_c(NiFe) vs spacer thickness for NiFe(300 Å)/SiO_2(x)/CoFe(300 Å) trilayers prepared by different methods.

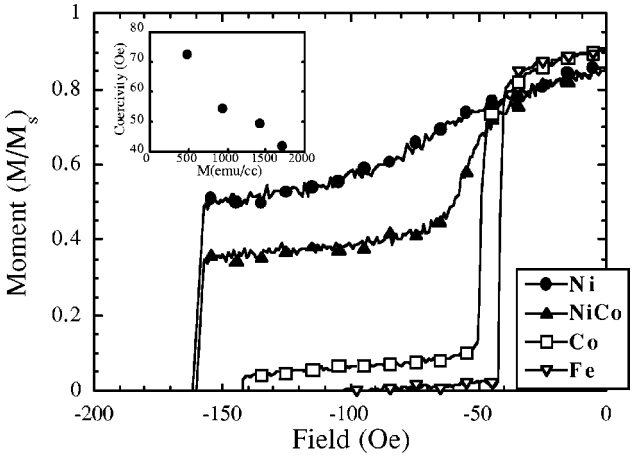

FIG. 7. Magnetization data (second quadrant) for FM(300 Å)/SiO_2(20 Å)/CoFe(300 Å) samples. The inset shows the H_c of the top layer (FM) vs top layer M.

the 20 Å spacer, but the relative increase in H_c with decreasing temperature was the same for both spacer thicknesses. Charge-mediated exchange[17] or exchange biasing,[18] which both should have a more rapid temperature dependence than observed, are therefore unlikely sources of the coupling. The increase in H_c(CoFe) with decreasing temperature was approximately linear, which suggests that strain may contribute to the temperature dependence. The same relative temperature dependence was observed in the free CoFe film. The temperature dependence of the free NiFe film coercivity was difficult to measure accurately due to the small values of coercivity.

C. Oxidation experiments

To investigate the permeable nature of thin sputtered layers of SiO_2, the deposition of trilayer samples was interrupted after the deposition of the oxide. At this stage, the SiO_2/CoFe bilayer was exposed to ambient atmosphere for 3 days. Afterward, the substrate was put back into the vacuum chamber for the NiFe deposition. The relative enhancement of H_c(NiFe) due to magnetic coupling was compared to trilayers grown *in situ*. For continuous, impermeable SiO_2 layers, no difference is expected. Figure 6 is a plot of H_c(NiFe) vs SiO_2 spacer thickness for trilayers grown by the two different procedures. For a spacer 10 Å thick, the NiFe coercive field decreased 8 Oe when the SiO_2/CoFe bilayer was exposed to atmosphere as an intermediate step. As the thickness of the SiO_2 layer increased, the difference in H_c(NiFe) between the different samples steadily decreased. In trilayers with at least 40 Å of SiO_2, H_c(NiFe) was independent of the deposition procedure, but was still enhanced compared to a free NiFe layer. These results indicate that the SiO_2 layer was permeable below 40 Å thick, allowing surface oxidation of the bottom CoFe layer. This oxidation diminished the coupling between the CoFe and NiFe films. Thus, the permeable nature of the SiO_2 may account for some direct magnetic coupling for small spacer thickness. As the data show, however, it is not the dominant mechanism for the enhanced H_c(NiFe).

D. Coupling between CoFe and other soft films

Coupling effects between CoFe and other soft magnetic films were also investigated. Ni, NiCo, Co, and Fe were used instead of NiFe. These films showed coercive fields of 20–25 Oe as free films but, like the NiFe, exhibited an enhanced H_c when placed in the trilayer structure with a CoFe film. Figure 7 shows the hysteresis loops (second quadrant) for a series of trilayers with various 300 Å thick films (FM) on top. The SiO_2 spacer was 20 Å thick, and 300 Å of CoFe was the base layer. The inset plots the top layer coercivity, H_c(FM), vs the top layer saturation magnetization, M(FM). As M(FM) increased, H_c(FM) *decreased*, and the moment reversal became sharper. The same trend of H_c(FM) with M(FM) was also observed with 100 Å SiO_2 spacers, so the direct coupling contribution does not appear to be significant. These results indicate that the coupling energy does not increase with M(FM).

E. Demagnetization experiments

The influence of the net CoFe moment on the coupling was probed with demagnetization experiments. Demagnetization was performed by cycling through hysteresis loops while progressively decreasing the maximum applied field. Figure 8 shows the NiFe minor loop behavior of a NiFe(300 Å)/SiO_2(20 Å)/CoFe(300 Å) trilayer under saturated and demagnetized CoFe magnetization conditions. When the CoFe film was saturated with a large positive or negative field and then left in the remanent state, the minor loops of the NiFe were asymmetric and shifted opposite to the direction of CoFe magnetization. After demagnetizing the trilayer, the NiFe minor loops were symmetric about zero applied field, but the enhanced H_c(NiFe) was still present. The same effects were observed for a sample with a 100 Å spacer. Since demagnetization eliminates the net moment, but domain walls remain, the persistence of the enhanced H_c(NiFe) after CoFe demagnetization suggests that CoFe domain walls are integral to the coupling.

IV. MÖSSBAUER POLARIZATION

Conversion electron Mössbauer spectroscopy measurements were made on trilayer samples to determine simulta-

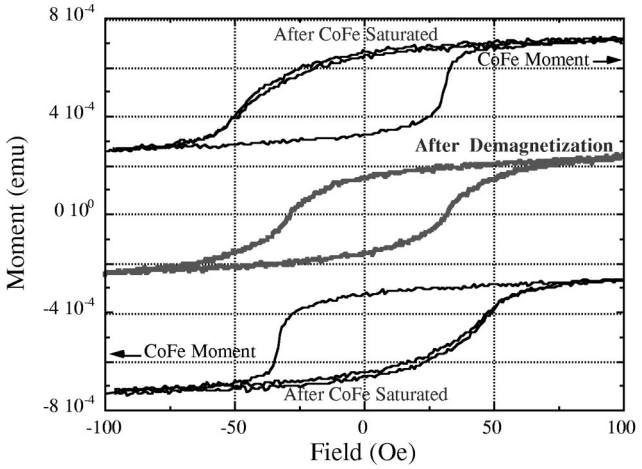

FIG. 8. Minor loops of the NiFe taken either before or after demagnetization of the CoFe in a NiFe(300 Å)/SiO_2(20 Å)/CoFe(300 Å) sample. Arrows denote the saturation direction of the CoFe.

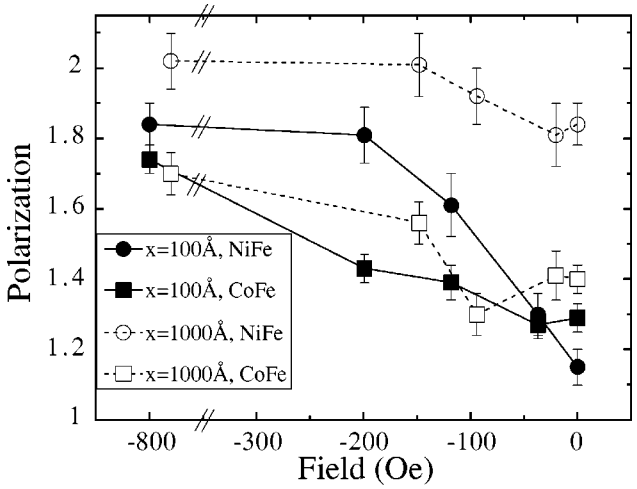

FIG. 9. Comparison of Mössbauer polarization vs applied field for the NiFe and CoFe layers in NiFe(300 Å)/$SiO_2(x)$/CoFe(300 Å) trilayers with either 100 or 1000 Å of SiO_2. Lines are visual guides.

neously the dispersion of spins in the individual magnetic layers along the nominal easy axis. Data were obtained with a He-CH_4 gas proportional detector and multichannel analyzer. A ^{57}Co (in Rh) source was used in two separate configurations that probed different characteristics of the in-plane magnetization distributions in both the NiFe and CoFe films. In one set of experiments, γ rays were directed perpendicular to the plane of the trilayer to detect the possible presence of spins out of the plane. In the other set of experiments, gamma rays were incident in the plane of the film (edge-on), but perpendicular to the nominal easy axis of the CoFe film to measure the in-plane dispersion of spins about the easy axis. In both sets of experiments, a field was applied along the easy axis in the plane of the film to cycle the trilayer through its hysteresis loop. The Mössbauer measurement gives information about the ^{57}Fe hyperfine fields. Due to the different hyperfine fields associated with each layer, the Mössbauer subspectra of the two layers were slightly shifted, separating the four outer peaks of each sextet. The relative intensities of the lines in each sextet are $3{:}2p{:}1{:}1{:}2p{:}3$, where p is the polarization. The polarization is dependent on θ, the angle between the incident γ-ray propagation direction and the Fe spin moment. For a uniform spin orientation, $p=2\sin^2\theta/(1+\cos^2\theta)$. A polarization factor of 2 means that the moments are completely perpendicular to the direction of the incident γ ray.

For measurements obtained with the γ ray directed perpendicular to the trilayers, each magnetic layer was found to have an in-plane spin orientation ($p=2$) for all applied field values. Within the limit of spins completely in the plane, a hypothetical value for p in the second geometry (γ ray directed in the plane of the film) was calculated for the limiting case where spins are random in the plane (or random in the upper half plane). This resulted in the value $p=2/3$. The other limit is complete collinear alignment ($p=2$) with the applied field axis.

Figure 9 shows the measured values of p vs applied field for two different trilayer samples in the second geometry. The NiFe and CoFe results are plotted for trilayers with 100 and 1000 Å of SiO_2 spacer material. The samples were first subjected to a saturating positive field (3 kOe). The measurements began at remanence and continued into the second and third quadrants of the hysteresis loops. The CoFe layer was never fully aligned in the field direction, even for fields up to 800 Oe. At H_c(CoFe) of the 100 Å spacer sample (160 Oe), there was no significant change in the polarization of the CoFe film. Likewise, there is little change in p(NiFe) at H_c(NiFe) (30 Oe) of the same sample. In fact, there was no difference at all found in the remanent values of p(NiFe) in separate minor loop measurements (not shown) obtained before and after the NiFe was switched in the second quadrant. The lack of change of p(NiFe) at H_c(NiFe) says that the NiFe is not strongly coupling to the vector magnetization of the CoFe, in agreement with the results of the demagnetization measurements. The NiFe layer showed a remanent spin orientation ($p=1.2$) similar to the value for the CoFe film ($p=1.3$) for the 100 Å SiO_2 spacer. These values of p are intermediate to the limiting cases discussed previously, indicating that both films were only partially aligned at remanence. In the 1000 Å spacer sample, however, the NiFe was nearly fully aligned in all applied fields. In that sample, H_c(NiFe) was only a few Oe greater than that of the free NiFe sample. The CoFe film exhibited about the same remanent polarization ($p=1.4$) as for the film in the trilayer with the thinner spacer.

V. MAGNETIC IMAGING

Lorentz TEM imaging was used to study the magnetic structure in single layer films and trilayers. The single layer NiFe and CoFe films displayed ripple structures composed of low angle domain walls due to the polycrystalline nature of the films. Images of a 300 Å thick NiFe film (with a 100 Å SiO_2 underlayer) are shown in Figs. 10(a)–10(d) for various points along its hysteresis loop. The hysteresis loop, as measured on an AGM, is also displayed with letters marking the approximate field value of each image. The magnitude of the vertical field (250 Oe) is not believed to be strong enough to affect the results significantly. The in-plane field, which is controlled by tilting the sample in the vertical field, runs

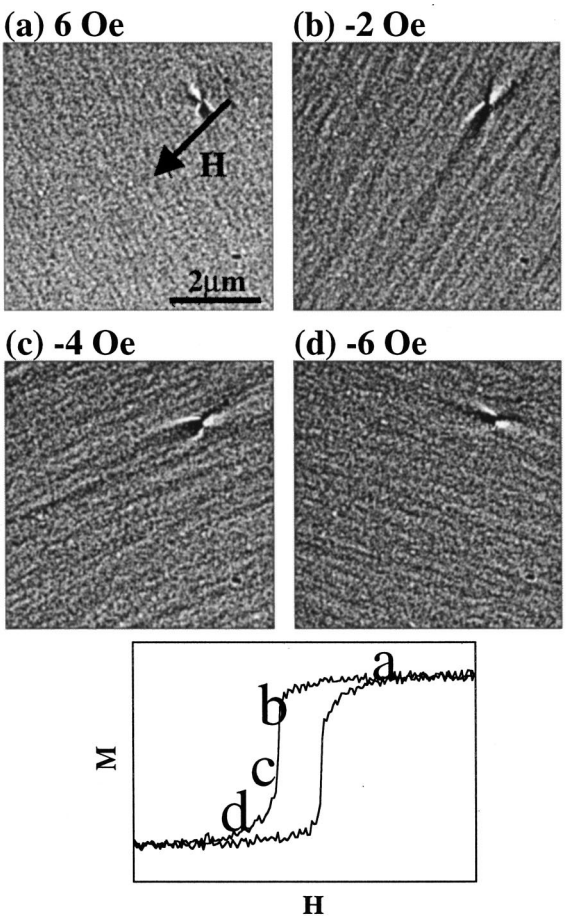

FIG. 10. Lorentz images of a 300 Å NiFe film in various applied fields along its hysteresis cycle.

diagonally from the top right to the bottom left corner of the images. The magnetic contrast features lie perpendicular to the magnetization direction due to the nature of the Lorentz force on the deflected electrons. The dark spot observable in the upper right-hand corner of the images is a defect in the film, useful for referencing magnetic features in other images. The NiFe showed free rotation of its ripple structure as its moment was reversed in a field of about 4–6 Oe. This value of H_c for the NiFe with a SiO_2 underlayer was larger than the 1 Oe H_c of the control samples grown on Si. This was typical of all samples grown on TEM grids. These grids are not as rigid as a Si substrate and often contain defects which may contribute to the slightly different coercivities.

The images from a CoFe film (Fig. 11) showed high contrast features associated with the magnetic ripple structure. At remanence and in fields smaller than H_c, many short wall segments appeared. The striking property of these wall fragments was that they were almost stationary [Figs. 11(c)–11(e)], changing only in contrast level until H_c was exceeded at ~140 Oe. Leading up to H_c, the wall fragments appeared to branch out and increase in contrast [Figs. 11(f) and 11(g)]. At H_c, a 180 degree domain wall was observed sweeping across the film. Even after the nominal H_c, some scattered regions of varying magnetic contrast were seen. The domain-wall behavior observed in the Lorentz images of the free CoFe film was consistent with its relatively isotropic and square hysteresis loops.

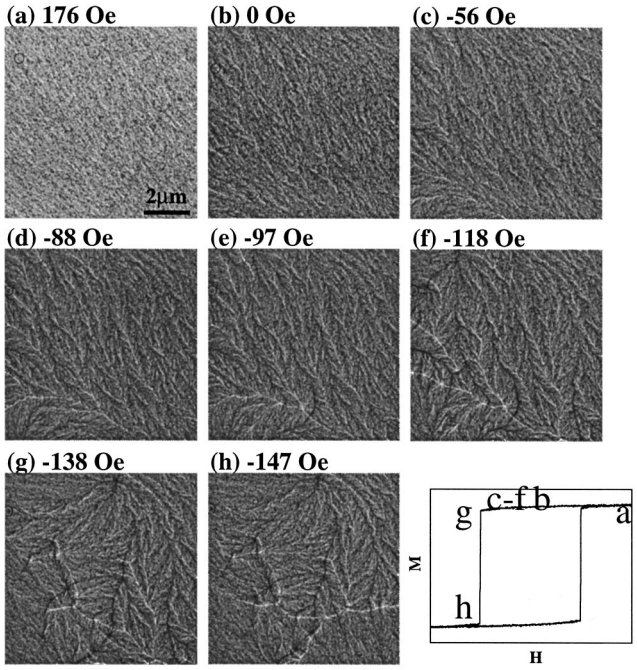

FIG. 11. Lorentz images of a 300 Å CoFe film in various applied fields along its hysteresis cycle.

The Lorentz images of the trilayer films showed the magnetic contrast from both films superimposed. This posed a challenge when trying to assign specific features to either film. The measured hysteresis loops were used to help analyze the images from two trilayers: one with 100 Å of SiO_2 spacer material and one with 1000 Å. Images of the trilayer with 100 Å of spacer are shown in Fig. 12. These images closely resemble those of the single CoFe layer, with some contrast changes attributable to the NiFe layer. An increase

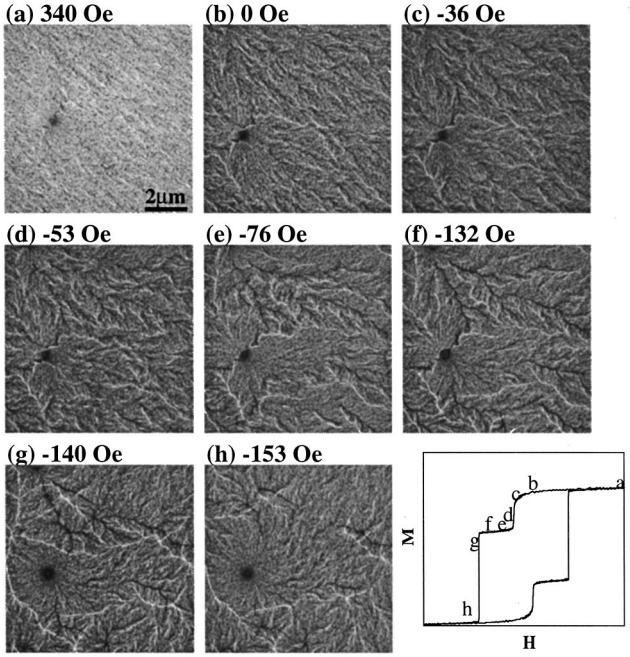

FIG. 12. Lorentz images of a NiFe(300 Å)/SiO_2(100 Å)/CoFe(300 Å) sample in various applied fields along its hysteresis cycle.

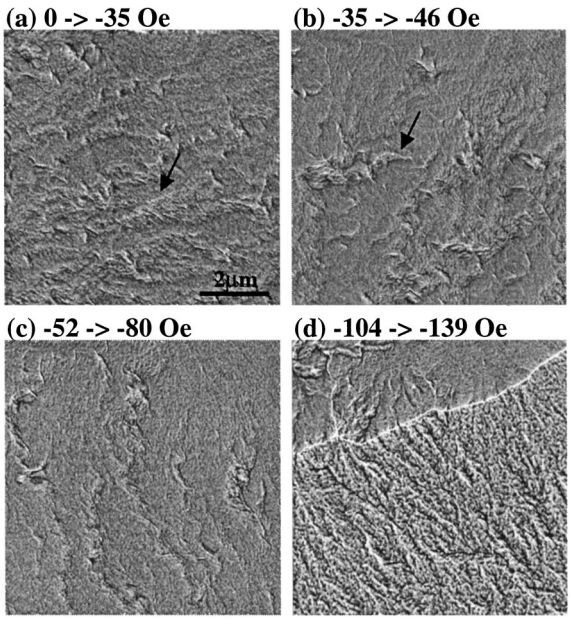

FIG. 13. Difference images reflecting changes in magnetic structure of a NiFe(300 Å)/SiO_2(100 Å)/CoFe(300 Å) sample. Arrows point to NiFe domain walls.

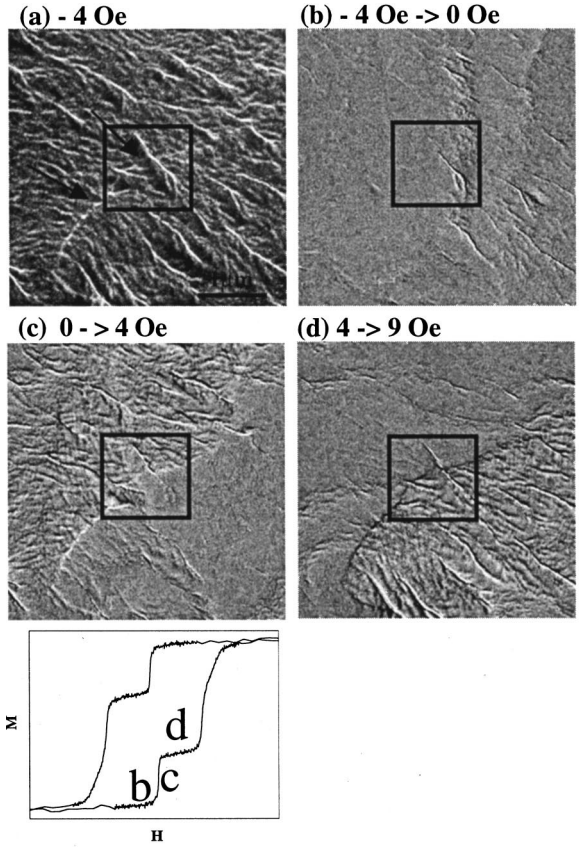

FIG. 14. (a) Lorentz and (b)–(d) difference images of a NiFe(300 Å)/SiO_2(1000 Å)/CoFe(300 Å) sample. Arrows point to a single NiFe domain wall.

in contrast of the various branching wall segments is noticeable at a smaller field [Figs. 12(b)–12(e)]. Figures 12(c) and 12(e) are images taken during the reversal of NiFe layer. The changing NiFe magnetization likely contributed to the changing contrast of the branching segments. The influence of the NiFe reversal on H_c(CoFe) was complicated, as evidenced by the irregular dependence of H_c(CoFe) on spacer thickness (see Fig. 2). Most of the high contrast features associated with the CoFe remained relatively rigid during the NiFe reversal.

Difference images of the 100 Å spacer sample (Fig. 13) were compiled by careful alignment and subtraction of one image from another taken at a higher field (from Fig. 12). These images are useful in detecting slight changes in the magnetic structure between points along the hysteresis loop. Besides statistical fluctuations and changing diffraction conditions in the crystallites as the sample is tilted, the contrast in these difference images arises from differences in the net deflection of the electron beam as it traverses the two magnetic layers. Unchanged regions appear with little or no contrast. The high contrast, bright/dark pairs of lines within the bands of lower contrast [Figs. 13(a)–13(c)] result from the altered deflection of the image of CoFe features due to localized magnetization rotation in the NiFe layer. For the imaging conditions used (defocus of 60 μm), it is expected that magnetic and nonmagnetic features in the CoFe layer will be shifted approximately 15 nm by magnetic deflection in the NiFe layer. Reversal of the NiFe would produce an apparent difference in position of 30 nm, as observed. The low intensity textured contrast in the bands cannot be assigned unambiguously to either layer. Figures 13(a) and 13(b) show difference images acquired around the coercive field of the NiFe layer (~30 Oe). The contrast in these images occurs in discrete bands indicating that the NiFe layer was not uniformly free to rotate over extended regions of the film but underwent a fragmented reversal process. Some of the single line features bordering the bands of contrast (indicated by arrows) are domain walls in the NiFe layer that were not seen in the single NiFe films. These walls were limited in length and occasionally appeared to be coupled with the immovable wall fragments of the CoFe [Fig. 13(b)]. Finally, at the coercive field of the CoFe layer (~130 Oe), a high contrast domain wall swept through the film, and the difference image [Fig. 13(d)] shows a much higher contrast in the texture of the reversed region (lower right-hand region). This is due to the changing magnetization of the CoFe layer.

By comparison, the trilayer with a 1000 Å spacer (Fig. 14) showed much longer walls, attributable to the NiFe layer, than the 100 Å spacer sample. Figure 14(a) shows a Lorentz image of the trilayer at 4 Oe with a box outlining a region where the NiFe wall intersects the ripple structure of the CoFe film. Arrows point to a long white wall about 100 Å wide that runs in the direction of the applied field but perpendicular to the CoFe high contrast ripple. Figures 14(b)–14(d) are the difference images for images taken around H_c(NiFe) (~9 Oe). These difference images show larger regions of the NiFe reversing for a given interval of the applied field, compared to the trilayer with a 100 Å spacer. As already discussed, the slight shift of the image of the CoFe walls produces bright/dark wall pairs in the difference images corresponding to regions where the NiFe is reversing. In Fig. 14(c), the high contrast features are in the upper left-hand corner since the NiFe has reversed in that region. The NiFe magnetization completes its reversal by sweeping through the bottom right-hand corner of Fig. 14(d). Of par-

ticular interest in Figs. 14(c) and 14(d) is the contrast in the outlined area, showing how the path of the NiFe wall responds to local coupling with CoFe ripple features. It is reasonable to still see coupling effects in this sample since even the trilayer with a 1000 Å spacer showed an increase in H_c(NiFe) compared to a free film.

VI. DISCUSSION

The Lorentz images showed that interlayer coupling was modifying the ripple structure and inducing domain walls in the NiFe films in the trilayers. A model was sought to describe the effective pinning of NiFe walls to the immobile walls in the CoFe. A precise model of H_c(NiFe) with spacer thickness (or thickness of magnetic layers, etc.) would require the consideration of how the shift in the NiFe minor loop adds to the observed coercivity. It has been demonstrated[19–22] that magnetostatic interlayer coupling can influence the types of domain walls in double NiFe films separated by SiO layers. In these studies, Néel walls were predominant in coupled NiFe films even for relatively large thicknesses that would normally contain only Bloch walls as free films. Quasi-Néel walls can be induced in one film to close the flux pattern from a Néel wall in the other film, allowing Néel walls to be energetically favorable in thicker films. In addition, coupled NiFe films showed smaller coercivities than free films. The decrease in H_c was attributed to a decrease in domain-wall energies because of the coupling.[19] In the present study, interlayer coupling changed the domain structure of the NiFe films. The modification of ripple structure and domain walls in the NiFe occurs to minimize the stray flux energy of the immobile walls in the CoFe.

The interaction of a stationary and a mobile domain wall was modeled by Fuller and Sullivan[13] in a trilayer system composed of two magnetic layers separated by a nonmagnetic, insulating material. They treated the walls as linear dipoles. The physical interpretation of such a model is that a sufficient field must be applied before the moving wall in the soft film can overcome the energy barrier imposed by coupling to the stationary wall in the hard film. The model predicted a decrease in the soft wall H_c with increasing spacer thickness, but the values of H_c were an order of magnitude larger than what was measured in this study. The model is oversimplified, however, assuming that domain-wall energies are much greater than the wall-wall interaction energies and neglecting how the coupling mechanism influences the characteristics of the walls themselves.[23]

Existent magnetostatic coupling models like Néel's ''orange-peel'' model and the dipolar wall coupling model cannot successfully explain all of our data. The wall coupling model can account qualitatively for the H_c(NiFe) dependence on spacer thickness (Fig. 2) and on CoFe layer thickness (Fig. 3). Neither model, however, can account for the H_c(NiFe) dependence on thickness of the NiFe layer (Fig. 4), or the soft layer H_c dependence on M of the soft layer (Fig. 7) because they assume a coupling energy density (E) that scales with the product of t and M of both magnetic layers. These models for the coercivity, however, require an assumption about the relationship between H_c(NiFe) and E. The simplest assumption is a ''lever-arm'' switching model for the NiFe layer, i.e., $E = H_c(\text{NiFe}) \times M(\text{NiFe}) \times t(\text{NiFe})$.[24] For those models, this results in an H_c(NiFe) that depends only on M and t of the CoFe layer. Our data (Lorentz and Mössbauer) show that the NiFe layer does not switch as a single layer, but switches in a fragmented fashion where different small regions are reversing in different fields. Thus, the simple ''lever-arm'' picture for reversal is not appropriate for modeling the coercivity. Nevertheless, the bulk of the data are consistent with a magnetostatic coupling associated with interacting domain walls. To adequately explain all of the data, the wall coupling model would have to be modified to take into consideration the *localized* interlayer coupling between walls and ripple structure and the influence of magnetic layer thickness on wall width. The Lorentz images showed that walls and ripple structure varied in both films with respect to wall spacing and length, angle between walls, and direction of wall propagation relative to the applied field. In addition, to explain the varying soft layer H_c data, the local anisotropy and magnetostriction in the soft film must be included.

VII. SUMMARY

We have investigated magnetic coupling phenomena between ferromagnetic thin films separated by an insulating layer. An enhanced soft layer H_c and shifted minor loops were observable even to quite large spacer thickness. The difference in H_c of a free NiFe film compared to one in the trilayer was attributed to magnetic coupling with domain walls in a hard CoFe film. SiO_2 layers less than 40 Å thick were permeable, allowing some direct coupling to increase H_c(NiFe). The lack of strong temperature dependence to the coupling, however, indicated that the dominant coupling mechanism had a magnetostatic origin. Demagnetization experiments favored domain-wall coupling as the primary mechanism. Mössbauer measurements confirmed that the NiFe spin dispersion was strongly influenced by the CoFe in cases of strong coupling, i.e., small spacer thickness. Imaging by Lorentz TEM revealed the formation of static domain-wall segments in the CoFe films that appeared to couple with induced walls and ripple structure in the NiFe in fields less than H_c(CoFe). For a trilayer with a 1000 Å spacer, the coupling effects were sufficiently reduced to allow large regions of the NiFe film to rotate freely. ''Orange-peel'' coupling is inconsistent with the data. A simple magnetostatic wall coupling model is also insufficient to explain all of the data. More detailed calculations are required to adequately model the complex localized nature of the interlayer coupling.

ACKNOWLEDGMENTS

This work was supported by NSF Grant No. DMR-9400439. Use of facilities at the Center for High Resolution Electron Microscopy at Arizona State University is gratefully acknowledged.

[1] M. N. Baibich, J. M. Broto, A. Fert, F. Nguyen Van Dau, F. Petroff, P. Etienne, G. Creuzet, A. Friederich, and J. Chazelas, Phys. Rev. Lett. **61**, 2472 (1988).
[2] W. P. Pratt, Jr., S. F. Lee, J. M. Slaughter, R. Loloee, P. A. Schroeder, and J. Bass, Phys. Rev. Lett. **66**, 3060 (1991).
[3] S. S. P. Parkin, R. Bhadra, and K. P. Roche, Phys. Rev. Lett. **66**, 2152 (1991).
[4] M. Julliere, Phys. Lett. **54A**, 225 (1975).
[5] R. E. Dunin-Borkowski, M. R. McCartney, David J. Smith, S. Gider, B.-U. Runge, and S. S. P. Parkin, J. Appl. Phys. **85**, 4815 (1999).
[6] S. Gider, A.-U. Runge, A. C. Marley, and S. S. P. Parkin, Science **281**, 797 (1998).
[7] C. C. Yu and A. K. Petford-Long, J. Appl. Phys. **85**, 5753 (1999).
[8] K.-S. Moon, R. E. Fontana, Jr., and S. S. P. Parkin, Appl. Phys. Lett. **74**, 3690 (1999).
[9] O. Massenet, F. Biragnet, H. Juretschke, R. Montmory, and A. Yelon, IEEE Trans. Magn. **2**, 553 (1966).
[10] L. Néel, Compt. Rendus **255**, 271 (1962); **255**, 1676 (1962).
[11] S. Demokritov, E. Tsymbal, P. Grnberg, W. Zinn, and I. K. Schuller, Phys. Rev. B **49**, 720 (1994).
[12] D. Wei and H. N. Bertram, IEEE Trans. Magn. **32**, 3434 (1996).
[13] H. W. Fuller and D. L. Sullivan, J. Appl. Phys. **33**, 1063 (1962).
[14] J. C. Slonczewski, Phys. Rev. B **39**, 6995 (1989).
[15] C. L. Platt, David J. Smith, M. R. McCartney, and A. E. Berkowitz (unpublished).
[16] B. D. Cullity, *Introduction to Magnetic Materials* (Addison-Wesley, Reading, MA, 1972), p. 432.
[17] B. Briner and M. Landolt, Z. Phys. B: Condens. Matter **92**, 137 (1993).
[18] A. S. Edelstein, R. H. Kodama, M. Miller, V. Browning, P. Lubitz, S. F. Cheng, and H. Sieber, Appl. Phys. Lett. **74**, 3872 (1999).
[19] F. J. Friedlaender and L. F. Silva, J. Appl. Phys. **36**, 946 (1965).
[20] F. Biragnet, J. Devenyi, G. Clerc, O. Massenet, R. Montmory, and A. Yelon, Phys. Status Solidi **16**, 569 (1966).
[21] J. C. Slonczewski and S. Middelhoek, Appl. Phys. Lett. **6**, 139 (1965).
[22] S. Middelhoek, J. Appl. Phys. **37**, 1276 (1966).
[23] H. W. Fuller and L. R. Lakin, J. Appl. Phys. **34**, 1069 (1963).
[24] D. Mauri, H. C. Siegmann, P. S. Bagus, and E. Kay, J. Appl. Phys. **62**, 3047 (1987).